

# Miniaturized Notched Ultra-Wideband Antenna Based on EBG Electromagnetic Bandgap Structure

Liang Zhang<sup>1, 2, \*</sup>, Shijie Huang<sup>1</sup>, Zhixiang Huang<sup>1</sup>, Changqing Liu<sup>1</sup>, Chao Wang<sup>1</sup>, Zhiwei Wan<sup>2</sup>, Xingchuan Yu<sup>2</sup>, and Xianliang Wu<sup>1</sup>

**Abstract**—This paper proposes a miniaturized monopole ultra-wideband antenna with single-frequency rejection. The recommended antenna size is reduced from  $58 \times 54 \text{ mm}^2$  to  $32 \times 54 \text{ mm}^2$  by the half-cut method. The bandgap design is achieved by placing a dual mushroom type electromagnetic bandgap (EBG) structure on the side of a coplanar waveguide feeding line. The equivalent circuit and surface current distribution were used to analyze and explain the effects of mushroom-like EBG cells and the principle of the half-cut method. Both the prototype antenna and the proposed antenna have been fabricated and tested. From the measurement results, the proposed antenna exhibits good band-stop characteristics and can reject the wireless LAN interference band (5.2 and 5.8 GHz bands). Furthermore, the proposed antenna has considerable gain over the entire operating frequency band except for the notch band.

## 1. INTRODUCTION

With the increasing demand for high-quality, high-speed, and high anti-interference signal transmission, the design of ultra-wideband (UWB) antennas has become one of the hot research spots in global wireless communication technology. Planar UWB monopole antenna has attracted the attention of many scholars as an important branch of UWB antenna. It has the advantages of a simple structure, low profile, omnidirectional radiation, etc. Many excellent UWB planar monopole antennas [1, 2] have been designed and studied; however, UWB antennas also have disadvantages. In the 3.1–10.6 GHz operating frequency band of UWB antennas, there are many narrow-band interference signals, which severely interfere with the performance of UWB systems. In order to eliminate the interaction between the systems, it is necessary to design a notch band in the working band of the UWB system. Hence, the research of a UWB antenna with a notch band is timely and of great significance. To achieve the notch function in a specific frequency band, several design methods of the UWB band-notched monopole antenna have been proposed [3–14], such as etch grooves [3–6] on the patch or ground plane, the addition of branches, and the introduction of DGS structures. Although these methods achieve the band-stop characteristics of a certain frequency band, they have great limitations, such as a cumbersome and complicated design process, and the traditional notch can cause distortion of the antenna pattern. As a special artificial electromagnetic material, an electromagnetic bandgap (EBG) structure can form a forbidden band in a certain frequency range due to its high impedance surface characteristics, so it can be used in the notch design of UWB antennas [12–18]. In this paper, by loading two parallel EBG structures on both sides of the coplanar waveguide (CPW) feeder, a notch is realized in the 5.150–5.825 GHz frequency band, which blocks the influence of signals in the wireless LAN (WLAN) system on the UWB system.

---

*Received 10 April 2020, Accepted 14 May 2020, Scheduled 27 May 2020*

\* Corresponding author: Liang Zhang (liangzh@hfnu.edu.cn).

<sup>1</sup> Key Lab of Ministry of Education of Intelligent Computing & Signal Processing, Anhui University, Hefei 230601, China. <sup>2</sup> An Hui Province Key Laboratory of Simulation and Design for Electronic Information System, Hefei Normal University, Hefei 230601, China.

Although this method solves the problem of interference of the narrowband system to the UWB system, its large size and bulkiness severely limits the application of the UWB antenna and does not conform to the development trend of miniaturization of the antenna. According to the working principle of a UWB antenna, the resonance frequency of an antenna is related to its size relative to the wavelength. A smaller relative size results in a higher resonance frequency, while a larger relative size results in a lower resonance frequency. For symmetrical UWB notch antennas, the structure along one side of the symmetry axis has all the necessary characteristics of the resonant frequency [19]. Therefore, half of the UWB notch antenna is expected to achieve the same bandwidth as the whole structure. If this solution is feasible, the size of the antenna will be greatly reduced, which has great advantages for further integration with the communication system. Based on the above principle and an analysis of the symmetry and the current distribution on the surface of the UWB notch antenna proposed in this paper, the symmetrical cutting method is used to cut the antenna. This method reduces the antenna size by more than 40%, while the performance remains almost unchanged. The proposed miniaturized UWB notch antenna has an impedance bandwidth of 2.6–12 GHz and realizes the notch band in the WLAN system, which has a good application prospect.

## 2. REFERENCE ANTENNA

The design of the CPW-fed monopole UWB notch antenna was achieved by printing the antenna on an F4B dielectric substrate with a relative dielectric constant of 2.65 and a thickness of 1 mm. The radiation patch, CPW feeding line, and floor were printed on the same side of the dielectric board. The main radiating patch consists of a half-elliptical patch, and the rectangular patches were combined. The radiating element was fed through the CPW coplanar waveguide, and two parallel mushroom-type EBG structures were placed on both sides of the CPW feeding line to achieve the suppression of the WLAN band. The specific structure is shown in Figure 1, and the parameters and their sizes are shown in Table 1.

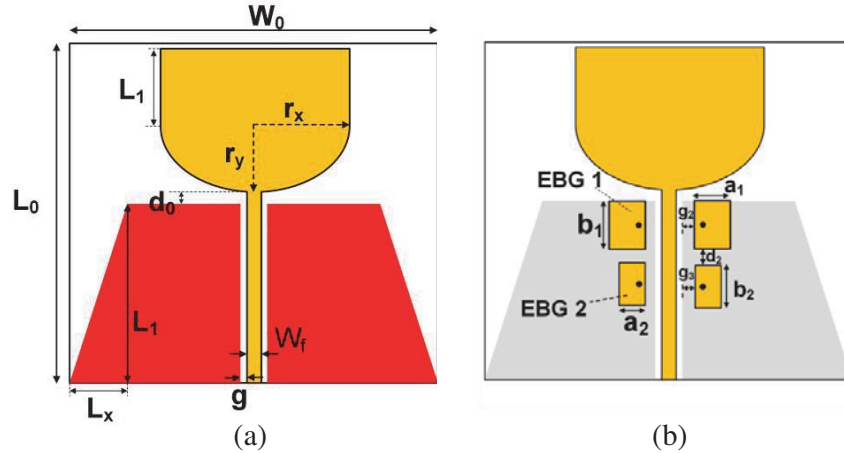


**Figure 1.** Schematic of prototype antenna. (a) Top view. (b) Bottom view.

The UWB printed monopole antennas were obtained from the planarization of cylindrical dipole antennas, and the initial size of the UWB antenna was determined by taking the correspondence between them. Changing the lengths of the long axis  $r_x$  and short axis  $r_y$  of the semi-elliptical patch and the height  $L_1$  of the rectangular patch can adjust the impedance bandwidth of the antenna. The antenna is given an input impedance of  $50 \Omega$  by setting the width  $W_f$  of the CPW feeding line and the interval  $g$ . A triangular plate is cut out from each of the two rectangular ground plates, and an appropriate wide-band characteristic can be obtained by properly selecting the size of the triangular plate.

The notch characteristics of the WLAN (5.10 GHz–5.88 GHz) band are obtained by loading two parallel EBG structures on both sides of the CPW feeder. As the notch bandwidth of a single EBG

**Table 1.** Dimensions of the prototype antenna.

Parameter	Length (mm)	Parameter	Length (mm)	Parameter	Length (mm)
$W_0$	58	$L_0$	54	$W_f$	2.5
$g$	2.2	$L_1$	30	$r_x$	15
$r_y$	11	$L_d$	3	$d_0$	0.1
$a_1$	4.3	$b_1$	10	$a_2$	3.3
$L_x$	9.3	$L_2$	12	$b_2$	10
$b_1$	10	$g_2$	0.1	$g_3$	0.1

structure is narrow and thus cannot satisfy the notch characteristics of the entire WLAN band, we placed two different sizes of mushroom EBG structures to block the entire WLAN band. The spacings  $g_1$  and  $g_2$  of the two EBG structures from the CPW feeding line are small, while the length of the EBG along the side of the CPW feeding line is long, thereby maximizing the coupling capacitance between the EBG unit and the feeding lines. Each EBG cell contains a rectangular patch and a short-circuit metal probe connecting the patch to the ground plane. The metal probe is 0.6 mm in diameter and is located on the side of the rectangular EBG cell near the CPW feeder. The distance between two EBG structures of different sizes is  $d_2$ .

The reason behind the notch characteristics of the electric band gap structure in some special frequency bands is the equivalence of the electromagnetic band gap structure to an LC filter circuit. The equivalent LC circuit of the dual mushroom type EBG structure is shown in Figure 2. It is shown that the resonance frequency of the EBG structure (that is, the center of the stopband frequency) can be calculated by the following formulae:

$$f_1 = \frac{1}{2\pi\sqrt{L1(C1 + C2)}} \tag{1}$$

$$f_2 = \frac{1}{2\pi\sqrt{L2(C3 + C4)}} \tag{2}$$

where  $C1$  and  $C3$  are the coupling capacitances between the EBG structure and the feeding line, and capacitances  $C2$  and  $C4$  are caused by the voltage difference between the patch and the ground plane. The current flowing through the hole generates the inductance  $L1$  and  $L2$ . The coupling capacitance ( $C1$ ), inductance ( $L1$ ), and parallel plate capacitor ( $C2$ ) can be approximated by the following expressions [15, 17, 18]

$$C1 = \frac{a_1\epsilon_0(1 + \epsilon_{eff})}{\pi} \cosh^{-1}\left(\frac{a_1 + g_2}{g_2}\right) \tag{3}$$

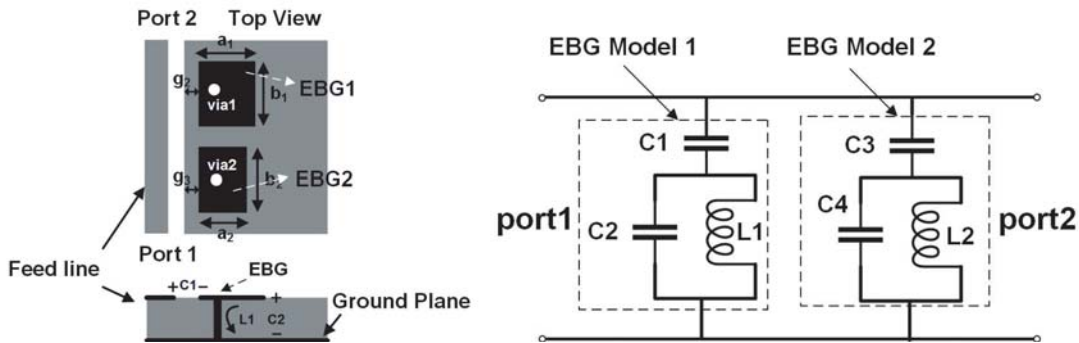


**Figure 2.** Equivalent LC circuit of EBG structure.

$$\varepsilon_{eff} = \frac{\varepsilon_r + 1}{2} + \frac{\varepsilon_r - 1}{2} \left( 1 + 12 \frac{h}{a_1} \right)^{-0.5}$$

$$L1 = \mu_0 h \quad (4)$$

$$C2 = \frac{\varepsilon_0 \varepsilon_{eff} a_1 b_1}{h} \quad (5)$$

where  $\varepsilon_0$ ,  $\mu_0$ , and  $\varepsilon_{eff}$  represent the permittivity, permeability of free space and the effective dielectric constant, respectively. Similarly, the formulae for capacitances  $C3$  and  $C4$  and the inductance  $L2$  can be obtained by substituting the relevant parameters into the above formulae. Two resonance frequencies are associated with EBG1 and EBG2, which occur at similar frequencies and merge with each other [16].

In order to get the required notch band, the values of  $C1$ ,  $C2$ , and  $L1$  can be regulated by changing the size of the first EBG structure so that the resonant frequency of the EBG unit is 5.25 GHz. The values of  $C3$ ,  $C4$ , and  $L2$  are adjusted by changing the size of the second EBG structure such that the resonant frequency of the EBG unit is 5.5 GHz, and a wide notch across the WLAN band (5.10 GHz–5.88 GHz) is achieved by the interaction of the two parallel EBG structures. Figure 3(a) shows the voltage standing wave ratio (VSWR) of the antenna after loading different sizes of EBG structure, where the parameters of each case are as follows: case 1:  $b1 = b2 = 12$  mm,  $a1 = 8$  mm,  $a2 = 7$  mm; case 2:  $b1 = b2 = 10$  mm,  $a1 = 4.3$  mm,  $a2 = 3.3$  mm; case 4:  $b1 = b2 = 8$  mm,  $a1 = 4$  mm,  $a2 = 3$  mm. Case 3 is a UWB antenna with an unloaded EBG, so we can obtain the stopband we need by loading different sizes of EBG structures. Figure 3(b) shows a comparison of the gains of the antennas loaded with (defined as antenna 1) and without (defined as antenna 2) the EBG in the direction of maximum radiation, indicating that loading the EBG is effective.

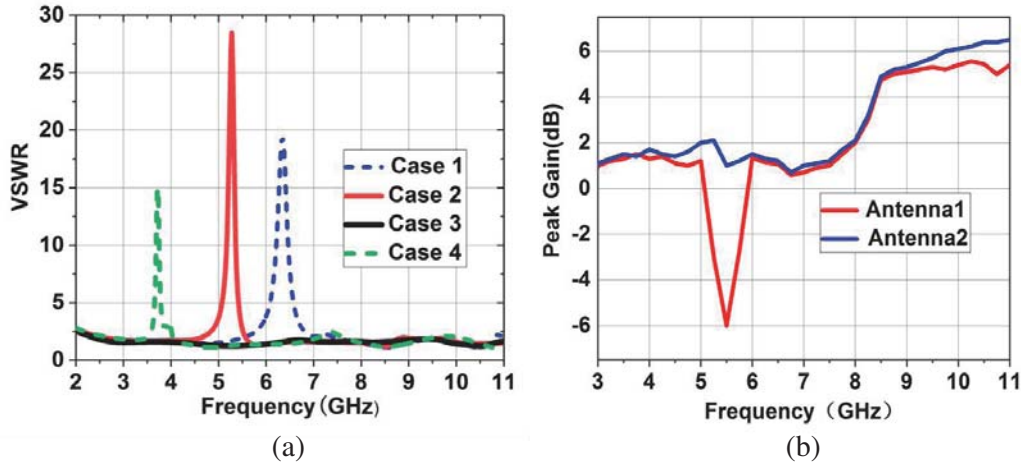


**Figure 3.** (a) Variation of VSWR with the variation of the size of the mushroom-like EBG patch. (b) Comparison of the peak gains of antenna 1 and antenna 2.

### 3. DESIGN OF THE MINIATURIZED UWB NOTCH ANTENNA

The method of achieving the miniaturization of the antenna is the focus of this investigation, and this section analyzes the UWB notch antenna proposed in the second section and uses the symmetrical cutting method to miniaturize the antenna. The structure of the UWB planar monopole proposed in Section 2 is symmetrical. According to the working principle of the UWB notch antenna described in the previous section, for symmetrical UWB notch antennas, the structure along one side of the symmetry axis has all the necessary characteristics of the resonant frequency. Therefore, it is expected that using just one half of the UWB notch antenna will be sufficient to achieve the same bandwidth as the whole structure. Based on this theory, we designed a miniaturized UWB band-notched monopole antenna, and the structure of this antenna is shown in Figure 4.

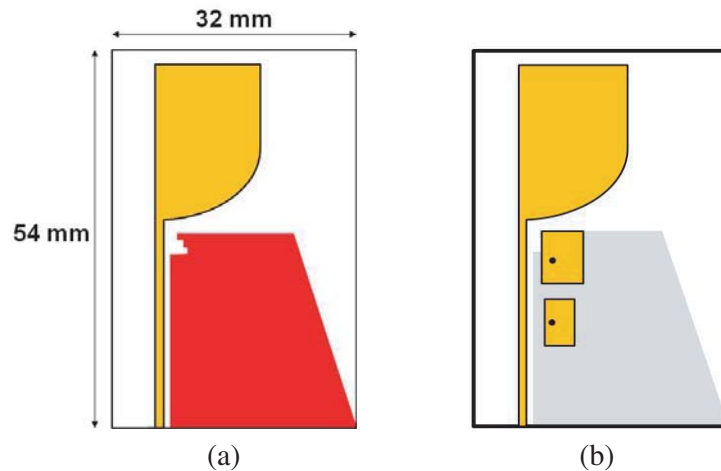


Figure 4. Schematic of the miniaturized notch UWB antenna. (a) Top view. (b) Bottom view.

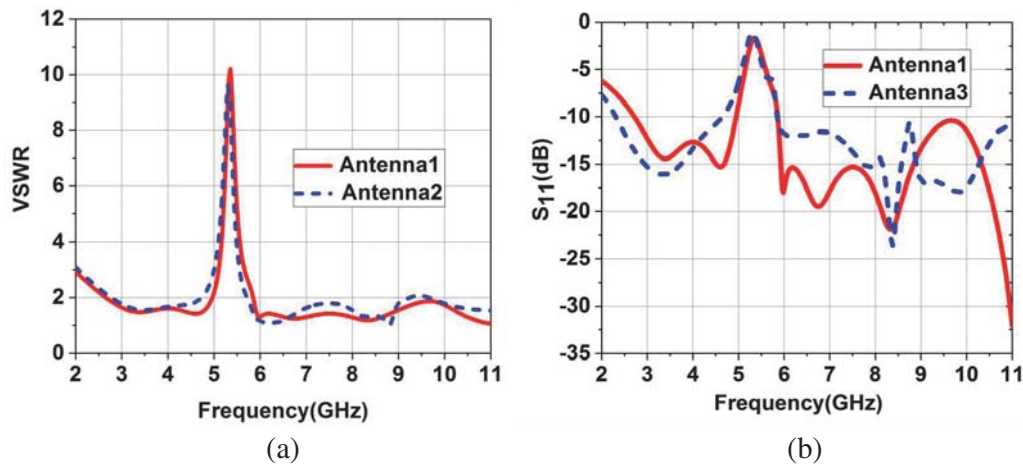
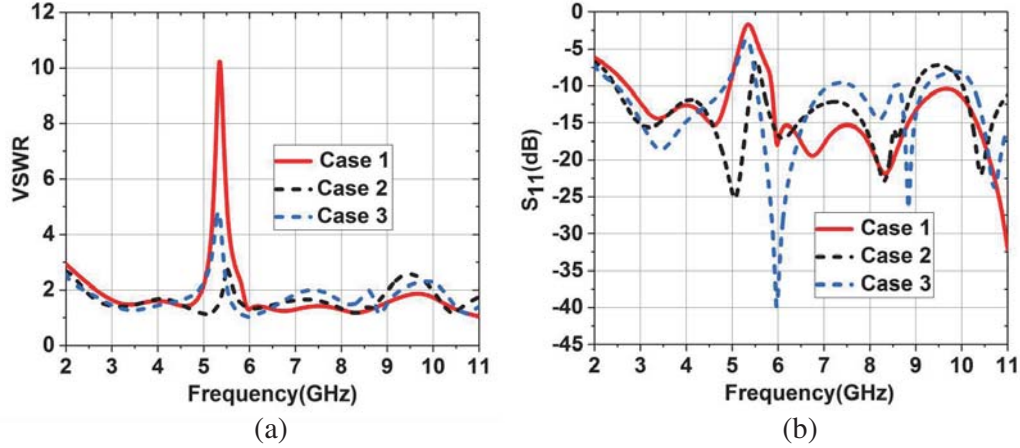


Figure 5. Comparison of the VSWR and  $S_{11}$  of antenna. (a) VSWR. (b)  $S_{11}$ .

The antenna is obtained by symmetric cutting of the prototype antenna proposed in Section 2. The radiating patch and ground plane are half of the original antenna. In order to facilitate the processing and fabrication of the antenna, we added a part of the dielectric substrate in the left half of the antenna. The size of the antenna is  $54 * 32 \text{ mm}^2$ , and the overall size is reduced by 40% of the original. The clipped antenna still maintains a good passband bandwidth and an excellent bandstop feature to block the influence of signals in the WLAN system. However, the reflection coefficient ( $S_{11}$ ) of the antenna after cutting is greater than 10 dB in a portion of the frequency band at around 9 GHz frequency. Therefore, we cut three small rectangular blocks with side lengths of 0.3 mm, 0.4 mm, and 0.5 mm in the upper right corner of the ground plane to increase the input capacitance at higher frequencies for impedance matching purposes [10]. Figure 5(a) shows a comparison of the VSWR parameters for an antenna (defined as antenna 1) after cutting a small rectangular block and an antenna (defined as antenna 2) of an uncut small rectangular block. Figure 5(b) shows the comparison of the  $S_{11}$  of the antenna after miniaturization (antenna 1) and the prototype antenna (defined as antenna 3).

The wide stopband effect of the dual EBG structure on the antenna can be verified by the results in Figure 6, showing the VSWR and  $S_{11}$  curves for the antenna in three cases: loading the parallel dual EBG structure (Case 1), separately loading the lower EBG structure (Case 2) and loading only the upper EBG structure (Case 3). It can be seen from the figure that the scheme of separately loading the upper EBG structure can only resist the interference of the lower half of the WLAN. Similarly, the



**Figure 6.** Comparison of the VSWR and  $S_{11}$  of Case 1, Case 2 and Case 3. (a) Simulated VSWR. (b) Simulated  $S_{11}$ .

scheme of separately loading the lower EBG structure can only resist the interference of the upper half of the WLAN. Loading two parallel EBG structures of different sizes can suppress the interference of the entire WLAN band to the UWB system.

Finally, the principle of the half-cut method is explained by the comparison of the surface current distribution of the miniaturized UWB notch antenna and the prototype antenna. Figure 7 shows the surface current distribution of the proposed antenna and prototype antenna at 3 GHz and 7 GHz. As shown in Figure 7, the miniaturized antenna and the right half of the prototype antenna have similar current distributions. This is because the CPW feed applies an even mode excitation to the non-miniaturized structure, where the mirror-symmetrical  $Y-Z$  plane acts as an open circuit (or magnetic wall). The removal of the left half of the non-miniature structure does not have a large effect on the current distribution of the right half, while the removal of the left half of the original structure does not greatly affect the current distribution of the right half. Therefore, the size of the antenna can be reduced by 40% without affecting the impedance bandwidth of the antenna by this method, and the space occupied by the antenna in the communication system is greatly reduced. Table 2 compares the results of this work with other UWB antennas with notch characteristics in the published literature, proving the effectiveness of the proposed method. To ensure a fair comparison, only antennas with similar substrate dielectric constants were chosen. In addition, the size of the antenna can be further reduced by using plates with higher dielectric constants in the antenna design.

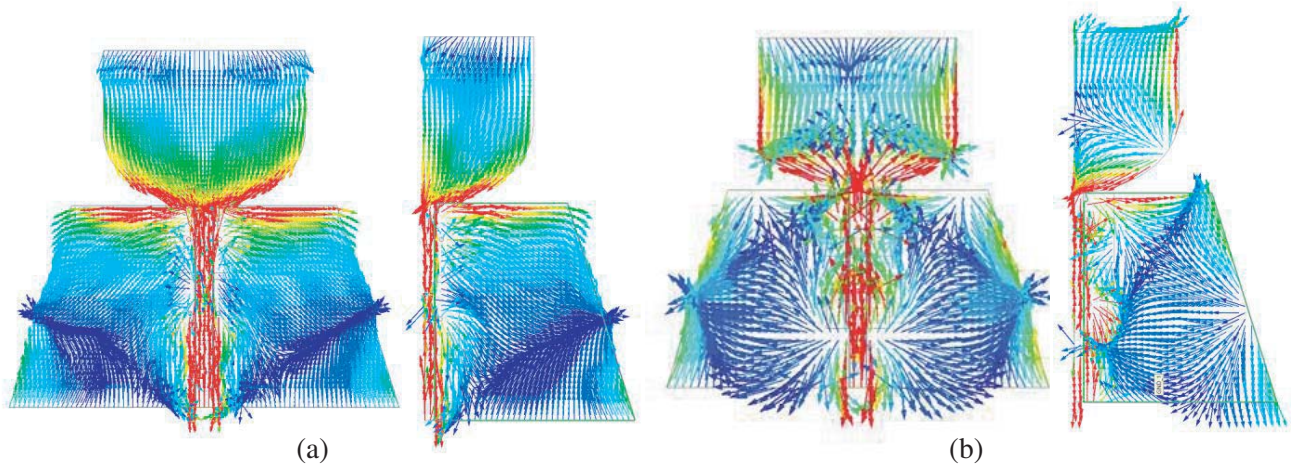


**Figure 7.** Comparison of surface current distribution between the miniaturized antenna and the prototype antenna: (a) at 3 GHz, (b) at 7 GHz.

**Table 2.** Performance comparison with published UWB antennas with notch characteristics.

Ref.	Dimensions (mm)	Dielectric constant	Notched-Band (GHz)
[16]	50 × 48	2.65	5.150–5.82
[13]	40.4 × 44	3.1	5.25–5.35, 5.725–5.775
[14]	50 × 50	2.33	5.33–5.34 7.9–7.95
work	54 × 32	2.65	5.150–5.825

#### 4. MEASUREMENT RESULTS

In order to further verify the performance of the miniaturized UWB notch antenna proposed in this paper, the miniaturized antenna and prototype antenna proposed in this paper were processed and tested. An image of the testing procedure of the antenna in a microwave darkroom is shown in Figure 8. The  $S_{11}$  of the proposed antenna was measured by an Agilent N5230A vector network analyser, and the results are presented in Figure 9(a). It can be observed that the  $S_{11}$  of the notch antenna is greater than  $-10$  dB in the 5.150–5.825 GHz band, indicating that the antenna has good notch characteristics

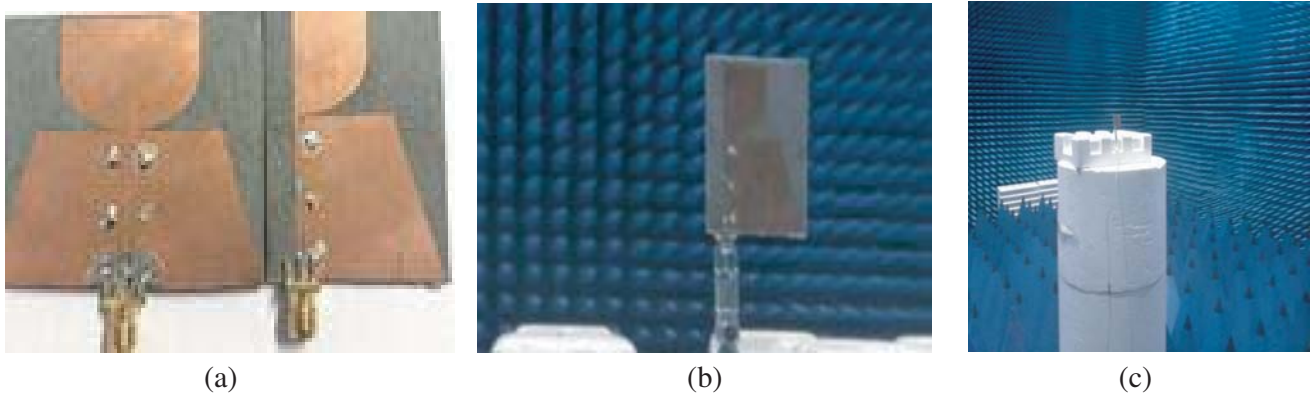


**Figure 8.** Antenna prototype and the measure environment. (a) The reference antenna and the miniaturized UWB notch antenna. (b) Antenna being tested in an anechoic chamber. (c) Far-field measuring platform.

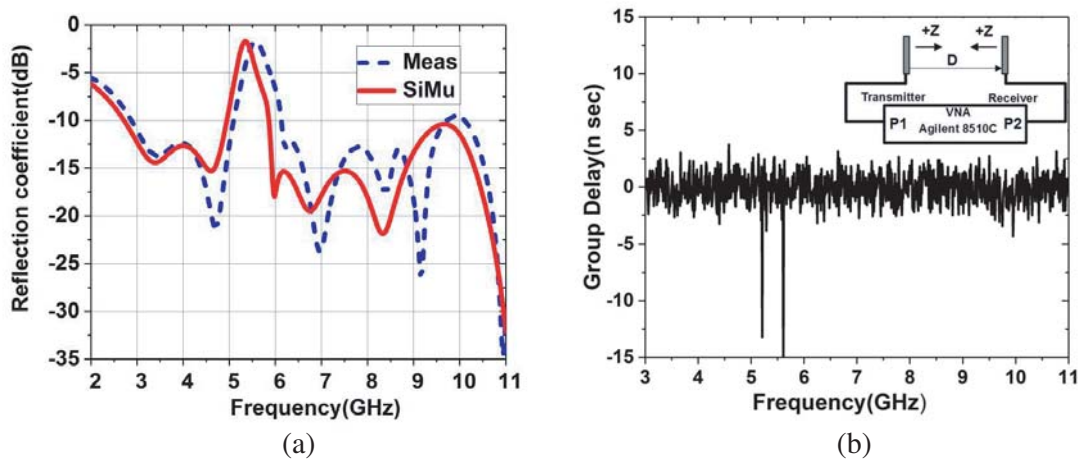


**Figure 9.** Measurements results of the proposed antenna. (a)  $S_{11}$ . (b) Group delay.

in the WLAN band.

Analysis of the group delay can show possible nonlinearities in the phase response and indicate the degree of distortion. For UWB applications, the group delay needs to be constant over the entire frequency band. The group delay of the proposed antenna is presented in Figure 9(b), measured on a pair of antennas designed in this work at a distance of 26 cm apart using an Agilent 8510C VNA. As shown in Figure 9(b), the variation of the group delay is small over the entire operating band apart from the notch band, which demonstrates that the proposed antenna has a good time-domain performance and minimal pulse distortion.

The radiation patterns at 3.5, 6.5, and 10 GHz are given in Figure 10, encompassing the upper, lower, and mid frequencies of the UWB. The radiation pattern on the  $H$ -plane was found to be almost omnidirectional at the operating frequency. At 3.5 GHz, the  $E$ -plane radiation pattern is similar to a monopole antenna, and changes can be observed at 6.5 GHz and 10 GHz. Moreover, the radiation patterns of the  $E$ -plane and  $H$ -plane were revealed to be stable over the entire operating frequency band. The measurement results are basically consistent with the simulation ones. The deviation between the two is mainly caused by the dielectric constant of the dielectric plate, the dimensional error of the antenna processing, the welding of the SMB joint, and the interference in the measurement environment, which render these deviations acceptable.

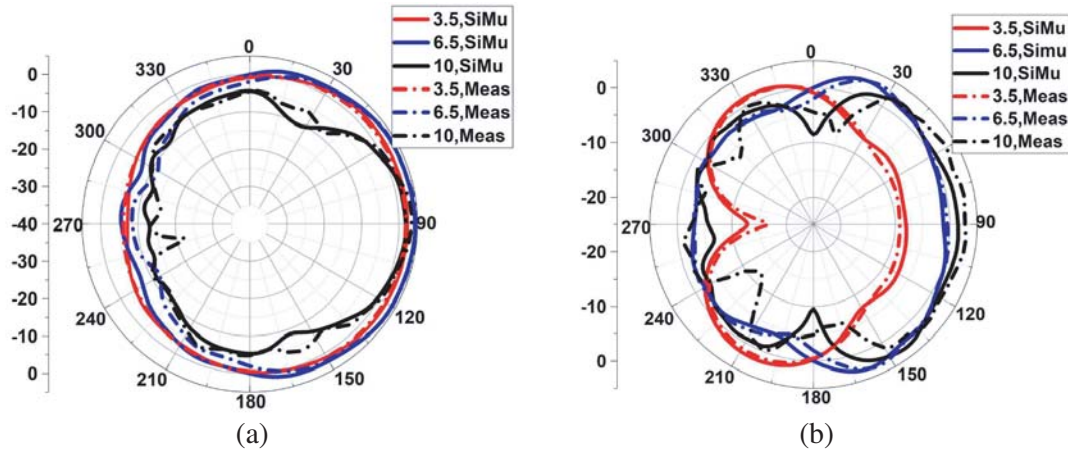


**Figure 10.** Simulated and measured far field radiation patterns. (a)  $H$ -plane (b)  $E$ -plane.

## 5. CONCLUSION

A new miniaturized UWB antenna was designed in this paper. By loading dual mushroom-type EBG structures on the side of the CPW feeding line, the wide notch characteristics of the antenna over the entire WLAN band (5.10–5.88 GHz) were obtained. The surface current distribution on the UWB filter antenna was analysed, and the size of the antenna was reduced by 40% using the symmetrical clipping method. Good radiation characteristics were maintained in the passband, which greatly facilitates the further integration of the UWB system.

## ACKNOWLEDGMENT

This research was partially supported by the Major Project of Provincial Natural Science Research of University of Anhui Province of China (Grant No. KJ2018ZD046), and the National Natural Science Foundation of China (Grant No. 61801163 and No. 61871001 and No. 61701003 and No. 61701001).

## REFERENCES

1. Jiang, D., Y. Xu, R. Xu, et al., "Compact dual-band-notched UWB planar monopole antenna with modified CSRR," *Electronics Letters*, Vol. 48, No. 20, 1250–1252, 2012.
2. Ojaroudi, M., G. Kohneshahri, and J. Noory, "Small modified monopole antenna for UWB application," *IET Microwaves Antennas & Propagation*, Vol. 3, No. 5, 863, 2009.
3. Sahoo, S., L. P. Mishra, M. N. Mohanty, et al., "Design of compact UWB monopole planar antenna with modified partial ground plane," *Microwave & Optical Technology Letters*, Vol. 60, No. 3, 578–583, 2018.
4. Avez, S. and R. W. Aldhaheri, "A Very Compact and Low Profile UWB Planar Antenna with WLAN Band Rejection," *Scientific World Journal*, Vol. 2016, 1–7, 2016.
5. Liao, X. J., H. C. Yang, N. Han, et al., "UWB antenna with dual narrow band notches for lower and upper WLAN bands," *Electronics Letters*, Vol. 46, No. 24, 1593, 2010.
6. Wang, J., Y. Yin, X. Liu, et al., "Trapezoid UWB antenna with dual band-notched characteristics for WiMAX/WLAN bands," *Electronics Letters*, Vol. 49, No. 11, 685–686, 2013.
7. Kim, C., H. Ahn, J. Kim, et al., "A compact 5 GHz WLAN notched bluetooth/UWB antenna," *2010 IEEE Antennas and Propagation Society International Symposium*, 1–4, Toronto, ON, Canada, 2010.
8. Oraizi, H., A. Amini, and M. Karimimehr, "Design of miniaturized UWB log-periodic end-fire antenna using several fractals with WLAN band-rejection," *IET Microwaves Antennas & Propagation*, Vol. 11, No. 2, 193–202, 2016.
9. Tang, Z., R. Lian, and Y. Yin, "Differential-fed UWB patch antenna with triple band-notched characteristics," *Electronics Letters*, Vol. 51, No. 22, 1728–1730, 2015.
10. Yadav, S., A. K. Gautam, B. K. Kanaujia, et al., "Design of band-rejected UWB planar antenna with integrated Bluetooth band," *IET Microwaves Antennas & Propagation*, Vol. 10, No. 14, 1528–1533, 2016.
11. Ghadimi, N. and N. Ojaroudi, "UWB small slot antenna with WLAN frequency band-stop function," *Electronics Letters*, Vol. 49, No. 21, 1317–1318, 2013.
12. Li, T., H. Q. Zhai, G. H. Li, et al., "Design of compact UWB band-notched antenna by means of electromagnetic-bandgap structures," *Electronics Letters*, Vol. 48, No. 11, 608–609, 2012.
13. Gheethan, A. A. and D. E. Anagnostou, "Dual band-reject UWB antenna with sharp rejection of narrow and closely-spaced bands," *IEEE Transactions on Antennas and Propagation*, Vol. 60, No. 4, 2071–2076, April 2012.
14. Siddiqui, J. Y., C. Saha, and Y. M. M. Antar, "Compact dual-SRR-loaded UWB monopole antenna with dual frequency and wideband notch characteristics," *IEEE Antennas and Wireless Propagation Letters*, Vol. 14, No. 1, 100–103, 2015.
15. Singh, R., G. K. Pandey, M. Agarwal, et al., "Compact planar monopole antenna with dual band notched characteristics using T-shaped stub and rectangular mushroom type electromagnetic band gap structure for UWB and Bluetooth applications," *Wireless Personal Communications*, Vol. 78, No. 1, 215–230, 2014.
16. Peng, L., B. J. Wen, X. F. Li, et al., "CPW fed UWB antenna by EBGs with wide rectangular notched-band," *IEEE Access*, Vol. 4, 9545–9552, 2016.
17. Peng, L. and C. L. Ruan, "UWB band-notched monopole antenna design using electromagnetic-bandgap structures," *IEEE Transactions on Microwave Theory & Techniques*, Vol. 59, No. 4, 1074–1081, 2011.
18. Mandal, T. and S. Das, "Design of a CPW-fed UWB printed antenna with dual notch band using mushroom structure," *International Journal of Microwave & Wireless Technologies*, 1–8, 2017.
19. Gao, G. P., B. Hu, and J. S. Zhang, "Design of a miniaturization printed circular-slot UWB antenna by the half-cutting method," *IEEE Antennas & Wireless Propagation Letters*, Vol. 12, No. 1, 567–570, 2013.